

Breakdown Processes in Nitrogen, Oxygen, and Mixtures*†

ELSA L. HUBER

Department of Physics, University of California, Berkeley, California †

(Received October 13, 1954)

The studies of corona mechanisms in coaxial cylindrical geometry with central anode using α -particle triggering, initiated by Colli and Facchini and by Lauer in inert gases, have been extended to pure nitrogen, pure oxygen, and mixtures of these gases. Pure gases were studied in a well outgassed system with nickel cathode. In pure nitrogen, from 25 to 600 mm pressure, the predominant mechanism is secondary liberation of electrons from the cathode by positive ion impact, with γ_i varying between 1.4×10^{-3} and 0.6×10^{-3} . Correction for back diffusion following Theobald gives a true γ_i of $2-3 \times 10^{-2}$. The ion is the N_2^+ observed by Varney, with reduced mobility 2.53 ± 0.08 cm²/volt sec at 760 mm and 20°C. Addition of the order of 1 percent oxygen reduces γ_i by a factor of $\frac{1}{2}$ and gives a weak photoelectric γ_p at the cathode, both effects resulting in part from action of oxygen on the cathode as noted by Parker and Theobald. Photoionization *in the gas* also appears, and with 5 percent oxygen the self-sustaining corona consists to a large extent of Geiger counter-like pulses propagating along the wire. In air, there is no longer any observable cathode action at threshold. With the use of transverse and longitudinal α particle trajectories relative to the axis, the velocity of propagation of the discharge down the wire has been measured for various pressures in air, and for constant pressure and potential as a function of oxygen concentration of between 5 and 20 percent. Velocities ranged between 10^8 and 10^7 cm/sec, decreasing as oxygen concentration increased. In pure oxygen above 200-mm pressure, the absorption of photoionizing radiation is so intense that, as indicated by Miller and Loeb, instead of spreading along the wire, the discharge propagates outward in the form of radial streamers, which have a duration of less than 10^{-7} sec, contain some 10^8 ions, and are spaced at regular intervals closely related to the positive-ion transit time. The latter yields a reduced mobility of 2.2 ± 0.1 cm²/volt-sec at 760 mm Hg and 20°C. in conformity with Varney's assumed O_2^+ ion.

INTRODUCTION

THE method developed by Lauer¹ from an earlier study of Colli and Facchini² for investigating the discharge mechanisms in a coaxial cylindrical system, with central wire positive, involved triggering the discharge by single α particles projected parallel to the axis of the electrodes. Such dynamic studies have proved so fruitful because of their high resolving power that the technique was extended to nitrogen, oxygen, and mixtures thereof. As had previously been shown with more primitive technique by Miller and Loeb,³ a wide variety of secondary mechanisms appear to occur in these gases. The excellent resolving power of the Lauer techniques thus offered a unique opportunity for direct visual and even quantitative study of the amazing sequence of breakdown phenomena in O_2 and N_2 mixtures as O_2 concentration increases.

APPARATUS AND PROCEDURES

The discharge tube was essentially that used by Lauer with the modifications noted. In order to minimize any leakage currents between the positive wire and the grounded cylinders via poor insulators, the platinum

anode wire was supported only from the ends of the glass envelope, with a tungsten spring at the lower end to maintain tension on the wire. After the cylinders had been mounted in the tube, the wire was aligned visually with two sets of mutually perpendicular marks on the outer rims of the two guard cylinders. A tungsten filament was provided outside the cathode cylinders for outgassing them by heating by electron bombardment.

The discharge was triggered by either of two α -particle sources. One source (longitudinal) furnished a beam of α particles parallel to the axis of the system and passing through the low-field region near the cathode. A second source (transverse) directed a beam between the upper two cylinders, perpendicular to the system axis but likewise passing through the low field region only. The α sources were constructed by plating polonium on the tip of a silver wire and inserting the wire 1 cm from the open end of a capillary tube 0.57 mm in diameter. This arrangement provided good collimation for the short trajectory of the transverse beam. For the longitudinal beam, a maximum deviation from the vertical of 3 mm was possible and could in some cases give rise to a slight variation in shape from one pulse to the next. Each source emitted approximately one α particle per second on the average. Pyrex shutters to which were attached slugs of soft iron could be operated by a small permanent magnet to turn the beams on and off.

For work with the pure gases nitrogen and oxygen, the discharge tube, which was mounted in an oven, was baked out at 450°C at least overnight, with mercury diffusion pump in continuous operation. Outgassing of the nickel cylinders consisted of heating them in

* This work was supported at various stages by both the U. S. Office of Naval Research and the National Science Foundation.

† This work has been presented in more detail in the Ph.D. thesis of Elsa L. Huber, Department of Physics, the University of California, Berkeley, California.

‡ Now at The University of California Radiation Laboratory, Livermore, California.

¹ E. J. Lauer, J. Appl. Phys. **23**, 300 (1952).

² L. Colli and U. Facchini, Phys. Rev. **88**, 987 (1952); L. Colli, Phys. Rev. **95**, 892 (1954); L. Colli and U. Facchini, Phys. Rev. **96**, 1 (1954).

³ C. G. Miller and L. B. Loeb, J. Appl. Phys. **22**, 494 (1951); **22**, 614 (1951); **22**, 740 (1951).

vacuum to a bright red heat for many hours by electron bombardment from the tungsten filament. The platinum filament was heated to a dull red for a few minutes by passing a current through it. The system was flushed with the purified gas to be used before filling.

Nitrogen was admitted into the system via a slow leak, then purified by passing it over potassium hydroxide pellets, then hot copper shot, and finally through a liquid nitrogen trap to remove carbon dioxide, oxygen, and water vapor, respectively. No difference in behavior was noted between Airco Prepurified Nitrogen (less than 0.002 percent oxygen) and Ohio's ordinary commercial variety when both were subjected to the purification described. Analysis by mass spectrometer of two samples of gas taken from the tube after purification indicated that flashing the W filament as a getter introduced more impurity than it removed.

In the case of oxygen extreme purity was less critically important than for nitrogen, so that after bakeout, outgassing, and flushing, ordinary tank oxygen was admitted at a fairly rapid rate, with the copper shot cold. Liquid nitrogen on the cold traps was replaced by dry ice-acetone baths.

The system was filled with room air also without any special precautions, except that again a dry ice-acetone mixture was used on the traps instead of liquid nitrogen to avoid condensing any of the oxygen. In addition to keeping mercury vapor out of the discharge tube, the cold traps helped insure uniform water vapor content of the air from one day to the next.

The signal from the discharge tube was picked up across a variable RC from the central collector cylinder to ground, amplified and observed on an oscilloscope, then recorded photographically. A Tektronix Type 511A synchroscope and Type 121 preamplifier (6×10^{-8} sec

rise time for the combination, 1×10^{-7} sec/cm maximum sweep speed) were adequate for most of the work. For the spreading velocity studies in air, which required a more rapid response, it was necessary to use the Type 517 Tektronix synchroscope, in conjunction with two Model 460A Hewlett Packard wide band amplifiers. The net rise time with this arrangement was 8×10^{-9} sec, with a maximum possible sweep speed of 10×10^{-9} sec/cm.

CHARACTERISTICS OF SECONDARY MECHANISMS

Reference may be made to Lauer's paper for details of some of the sequence of mechanisms observed. To facilitate the reading certain features must be recalled. The α particle creates n_0 electrons and ions near the outer cathode cylinder. At appropriate fields the fine linear electron cloud crosses to the anode in a transit time τ_e . On its way each electron produces an avalanche of $M = \exp(\int_b^a \alpha dr)$ electrons, where α is the first Townsend coefficient, r is the radial distance, and a and b the radii of anode and cathode respectively. Absorption of electrons by the anode discloses in the gap, but near the anode wire, the space charge of positive ions left by the avalanche. This induces a current flow from ground to cathode leading to an initial sharp pulse on the oscilloscope. This is the primary and triggering mechanism. The positive ions drift to the cathode in a time τ_i leading to a decline of the current pulse to zero on arrival. The avalanche of electrons, ions, and excited molecules results in three possible secondary mechanisms: (1) Positive ions on arrival at the cathode liberate electrons in virtue of their potential energy with a chance γ_i per ion. (2) Photons of sufficient energy which reach the cathode without resonance absorption liberate photoelectrons with a chance γ_p for the photon production accompanying each ion created in the avalanche. (3) Photons of sufficient energy but highly absorbed may cause photoionization of the gas which under appropriate circumstances will either propagate a discharge along the anode wire (*burst pulse*) or radially outward (*streamer*). Both of these self-sustaining discharges yield many electrons but ultimately quench by space charge. Process 1 is characterized by a succession of one or more secondary pulses following the primary one spaced $\tau_e + \tau_i$, or about a few hundred microseconds, apart. Process 2 is characterized by one or more secondary pulses spaced τ_e , or about a microsecond, apart. Process 3 will lead to pulses which are large, independent of triggering, above 100 microseconds long, and are irregularly spaced for burst pulses, but may be regularly spaced, very short, and with heavy ionization for streamers. Secondary liberation by entrapped radiation or by diffusion of metastable configurations to the cathode will be too slow and diffuse to record on the oscilloscope as used. Attachment of electrons to molecules to give negative ions will lead to irregular delayed pulses between τ_e and τ_i in time.

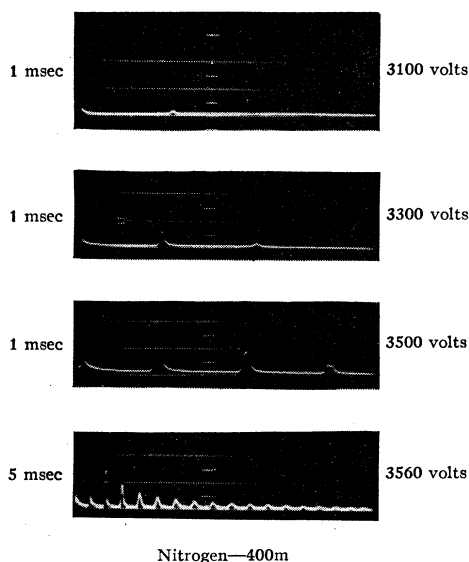


FIG. 1. Secondary ion pulses in pure nitrogen, 400 mm Hg, $RC = 3 \mu\text{sec}$; single sweep.

RESULTS AND DISCUSSION

Pure Nitrogen

The behavior of pure nitrogen was uniform over the entire pressure range studied, from 25 to 600 mm. As the voltage across the tube was gradually raised, the initial pulse representing the primary avalanche formation was followed by first one, then more and more secondary pulses. Figure 1 shows a representative set of oscillograms taken at a pressure of 400 mm. The secondary pulses were spaced at uniform intervals from the first at a given voltage and pressure. Consecutive pulses within one sequence showed a gradual decrease in amplitude, the decrease, however, becoming less pronounced as the onset voltage for a self-sustaining discharge was approached. The lower trace photograph was taken at 10 volts below onset.

Spacing between regular pulses corresponds to one ion transit time from wire to cylinder, indicating that the important secondary mechanism is electron liberation from the cathode by positive ion impact. With a faster sweep speed adjusted to τ_0 , there was no indication of any photoelectric action at the cathode. The smooth shape of the ion pulses indicates secondary electron production in the gas to be negligible.

The spacing between pulses yielded the ion mobility. Data were reduced to mobilities as by Lauer, no space charge correction being required. The plot of the reciprocal mobility against pressure was strictly linear. Extrapolation of the resulting straight line gave a value of 2.53 ± 0.08 cm²/volt-sec at 760 mm Hg and 20°C. The work of Varney on nitrogen mobilities⁴ and the mass spectrographic studies of Luhr⁵ indicate that the ion involved is N₄⁺, a conclusion supported by the fit of the measured mobility to the mass dispersion curve⁶ for positive ions in nitrogen.

From the oscillograms it was also possible to determine the magnitude of γ_i , the number of secondary electrons per incident positive ion released at the cathode as indicated by Lauer using n_0 and M .

The amplification factor $M = n/n_0$ was determined as follows: n could be obtained directly from the oscillograms by measuring the area under the primary pulse. At the maximum available gain, an observable deflection could not be obtained for the n_0 ions collected with no multiplication, and n_0 was therefore estimated from the known ionization of an α particle. Relative stopping power for nitrogen and oxygen are nearly the same (1.07 for oxygen with respect to 1.00 for air).⁷ On the assumption that specific ionization is proportional to pressure, range-energy curves for α particles in air⁸ were therefore used to find the energy lost over the 6-cm

TABLE I. Secondary emission coefficient for nitrogen ions on nickel.

p (mm Hg)	(a) M_{meas}	(b) $1000\gamma_i$ (M_{calc})	(c) $(E/p)_{\text{max}}$	(d) $100j/j_0$	(e) $100\gamma_i'$
600	0.6	0.7	220	3.0	2.0
500	0.7	1.0	230	3.1	2.3
400	1.1	1.2	250	3.4	3.2
300	1.0	1.3	290	3.7	2.7
200	1.2	1.5	360	4.1	2.9
100	1.5	2.4	530	5.9	2.5
50	1.4	3.4	780	6.9	2.0

length of the center cylinder. This implies that where the track range extended beyond the center cylinder adequate correction was made. n_0 was then given by the ratio of this energy loss to the 35 ev required per ion pair.⁷ Column (a) of Table I lists the resulting values of γ_i . Various other methods for calculating M , as indicated by Lauer and later by Colli and Facchini,² were used as checks. Accuracy at best was ± 20 percent.

In this study, only electrons that escape back-diffusion to the cathode can participate in secondary avalanches and contribute to the measured γ_i . In order to determine the γ_i' that would be measured if all the secondary electrons escaped, correction was made following the procedure of Theobald.⁹

Column (d) of Table I lists j/j_0 as calculated from the Thomson⁹ equation, and column (e) the corrected values of γ_i' . The data of Nielsen¹⁰ were used to obtain the electron drift velocities v corresponding to the values of E/p at the cathode. The average energy of emission of the secondary electrons has been estimated at 3 ev, based on the mechanisms which have been proposed to describe electron ejection from a metal surface by slow positive ions.¹¹

The corrected values of γ_i' could well be in error by a factor of 2 because of the approximations involved. No other measurements have been reported specifically for N₄⁺ with thermal energy on nickel, but there is satisfactory agreement in order of magnitude with the results of other authors^{12,13} for ions having ionization energies close to that of N₄⁺, incident on metals with work functions similar to that of nickel.

Effect of Few Percent Oxygen in Nitrogen

With the addition of a few percent oxygen to the nitrogen, a number of distinct changes occurred:

1. The secondary pulses from γ_i were smaller and fewer in number at a given V and p than in pure nitrogen.

⁴ R. N. Varney, Phys. Rev. **89**, 708 (1953).

⁵ O. Luhr, Phys. Rev. **44**, 459 (1953).

⁶ A. M. Tyndall, *The Mobility of Positive Ions in Gases* (Cambridge University Press, London, 1938).

⁷ F. Rasetti, *Elements of Nuclear Physics* (Prentice-Hall Publications, New York, 1936).

⁸ H. A. Bethe, "The Properties of Atomic Nuclei," AEC, Oak Ridge Tenn. (1949) (unpublished).

⁹ J. K. Theobald, J. Appl. Phys. **24**, 123 (1953).

¹⁰ R. A. Nielsen, Phys. Rev. **50**, 950 (1936).

¹¹ H. D. Hagstrum, Phys. Rev. **89**, 244 (1953). Also private communication on need for heating to 900°C or more to remove contamination by exposure.

¹² J. H. Parker, Phys. Rev. **93**, 1148 (1954).

¹³ J. P. Molnar, Phys. Rev. **83**, 940 (1951).

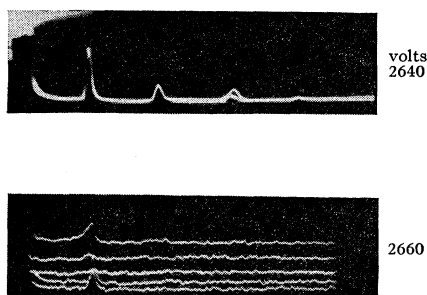


FIG. 2. Secondary ion pulses, top trace, and self-sustaining discharge in pure nitrogen, 200 mm Hg, 1000 μ sec full scale, $RC = 3 \mu$ sec. Upper trace—a few superposed sweeps. Lower trace—several single sweeps separated by vertical displacement showing initial and secondary with self-sustaining fluctuation.

2. The secondary pulses from γ_i began to lose their smooth shape and became rather ragged.
3. Onset of a self-sustaining discharge occurred at a voltage approximately 10 percent higher than in pure nitrogen.
4. With a faster sweep speed and shorter circuit RC , a new type of secondary pulse was observed, spaced at intervals of about a microsecond from the primary.

The above effects are illustrated in the photographs of Figs. 2, 3, and 4, all taken at a pressure of 200 mm. Figure 2 shows the ion secondaries in pure nitrogen at

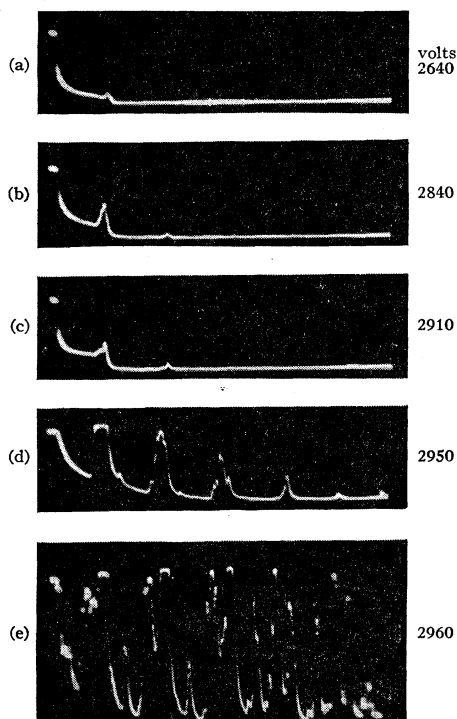


FIG. 3. Secondary ion pulses and self-sustaining discharge in nitrogen plus 5 percent oxygen, 200 mm Hg, 1000 μ sec full scale, $RC = 3 \mu$ sec. Traces such as *d* and *e* are single sweeps.

2640 volts and the self-sustaining discharge starting at 2660 volts. Comparison may be made with Fig. 3 for nitrogen plus 5 percent oxygen. In 3(a), barely one ion secondary can be seen at 2640 volts as opposed to four in pure nitrogen. Onset, as shown in 3(e), does not occur until V is raised to 2960 volts, 300 volts higher than in pure nitrogen. 3(b), (c), and (d) show how the ion pulses, while still clearly present, become progressively more irregular as the voltage is raised to onset. Compare the fluctuations of 3(e) with those in the lower trace of 2. The microsecond pulses are illustrated in Fig. 4.

It thus appears that there is a reduction in γ_i by a factor of approximately 5 with 5 percent O_2 over that of N_2 . The change in γ_i is associated with an increase in the work function of the surface and a change in the secondary emission mechanism, as discussed by Parker,¹² who found at low ion energies for A^+ on platinum and tantalum that γ_i decreased by an order of magnitude if the cathode was treated with oxygen instead of nitrogen. That this change is a cathode phenomenon and not one due to possible change in ions was checked by removing the O_2 and refilling with pure N_2 . Restoration of the initial γ_i on clean Ni did not occur until the cathode was heated to 900°C for hours in conformity to the experience of Hagstrum,¹¹ Parker¹² and recently Colli and Facchini² on this apparatus.

The microsecond pulses show the presence of a photoelectric γ_p in this mixture, absent in pure N_2 , which is confirmed by the fact that the spacing of these fast pulses corresponds to an electron transit time in order of magnitude. These pulses are smeared and irregular compared to those of Lauer in H_2 . It may therefore be concluded that these pulses represent secondary electrons released from the cathode by photons created in the preceding set of avalanches with, perhaps, some delay. Electron transit times were calculated by numerical integration of Nielsen's data¹⁰ for electron drift velocity as a function of E/p in nitrogen.¹⁴ Comparison between the measured τ_e , based on spacing between the microsecond pulses, and the calculated values is made in Table II. It is to be noted that these pulses, unlike those of Lauer in H_2 , do not give a self-sustaining discharge at 2960 volts where the slower sweep pulses are self-propagating.

Absence of a cathode photoelectric effect in pure nitrogen may involve capture of photons by resonance absorption, or simply a difference in the photosensitivity of the cathode. The present results in any case agree with the observations of Burch, Irick, and Geballe,¹⁵ who found an order of magnitude increase in the photoelectric yield from the cathode in a nitrogen-4 percent oxygen mixture and in air over that in either pure nitrogen or pure oxygen.

¹⁴ To justify comparison with data taken in pure nitrogen, measurements were made on photoelectric pulses obtained with minimum possible oxygen concentration of about 1 percent.

¹⁵ Burch, Irick, and Geballe, 1953 Conference on Gaseous Electronics, Washington, D. C., October 22-24, 1953 (unpublished).

The attachment of electrons to O_2 molecules to form negative ions and their subsequent detachment in the high fields near the anode to start delayed avalanches could account for an increase in pulse duration and small fluctuations in pulse amplitude. (See work of Lauer¹ in hydrogen with 0.1 and 1 percent oxygen.) However, the pronounced irregularities in pulse shape evident in Fig. 3(d), for example, cannot be explained in terms of negative-ion formation, but represent creation of secondary electrons by photoionization of gas molecules. With 5 percent oxygen, moreover, the oscilloscope pattern characterizing onset differs markedly from that in pure nitrogen. In Fig. 3(e) there is still some slight evidence of secondary ion pulses, but in addition, an indication that the discharge is being quenched, apparently along the entire length of the wire, at intervals shorter than an ion-crossing time. Such behavior would be characteristic of the burst pulse phenomenon described in detail by Loeb,¹⁶ in which the discharge spreads along the wire by photoionization of gas molecules, burns until sufficient positive ion space charge accumulates to lower the field at the wire and decrease the multiplication, and thus is finally choked

TABLE II. Comparison between measured and calculated electron transit times in oxygen-contaminated nitrogen.

p (mm Hg)	τ_e (μ sec)	
	Measured	Calculated
600	0.96	0.98
400	0.88	0.87
200	0.68	0.69
100	0.48	0.51
50	0.35	0.38

off. This action is also the one responsible for the discharge in fast Geiger counters. With clearing of the space charge the field recovers, and a new discharge can start somewhere along the wire length and again propagate along the high-field region by photoionization.

Nitrogen Plus 20 Percent Oxygen

Figure 5 illustrates another marked change in the character of the discharge mechanism that occurred when the oxygen concentration was increased to 20 percent. Below onset, the α -particle triggering produced irregular "bursts" of ionization, as shown in 5(a) and (b), which resemble the burst pulses first observed by Trichel¹⁷ and Kip¹⁸ in positive point-to-plane corona in air, and also noted by Miller³ with cylindrical geometry. At onset the discharge went over into steady burst pulse corona, illustrated in Fig. 5(c).

There was no indication whatever of secondary electron production at the cathode, either by ions or photons. Nevertheless, the discharge became self-sustaining at

¹⁶ L. B. Loeb, Phys. Rev. **73**, 798 (1948).

¹⁷ G. W. Trichel, Phys. Rev. **55**, 382 (1939).

¹⁸ A. F. Kip, Phys. Rev. **54**, 139 (1938); **55**, 549 (1939).

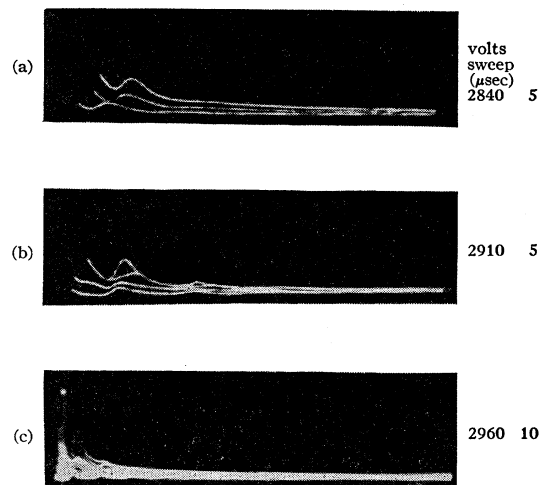


FIG. 4. Secondary photoelectric pulses in nitrogen plus 5 percent oxygen, 200 mm Hg, $RC=0.03 \mu$ sec. Several sweeps indicate lack of accurate reproducibility and that at self-sustaining corona in trace (c) the photon γ_p does not sustain itself as a discharge.

2145 volts, appreciably lower than in either pure nitrogen or nitrogen with a few percent only of oxygen. This lowering of the onset potential indicates a marked increase in the production of secondary electrons in spite of the absence of a γ action at the cathode, the predominant secondary mechanism in this case being photoionization of gas molecules, with alternate propagation along the wire and space-charge quenching of the discharge, as described in the preceding section.

Spread of the Discharge Along the Wire in Air

The object of this part of the work was to establish that the spreading process does occur in dried room air,

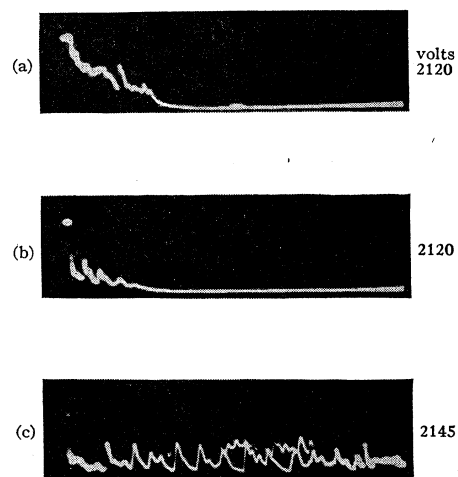


FIG. 5. Burst pulses and self-sustaining discharge in nitrogen—20 percent oxygen mixture, 200 mm Hg, 1000 μ sec full scale, $RC=3 \mu$ sec. Gain is down by a factor of 10 in (c). Single sweeps, except part of a second sweep in (c).

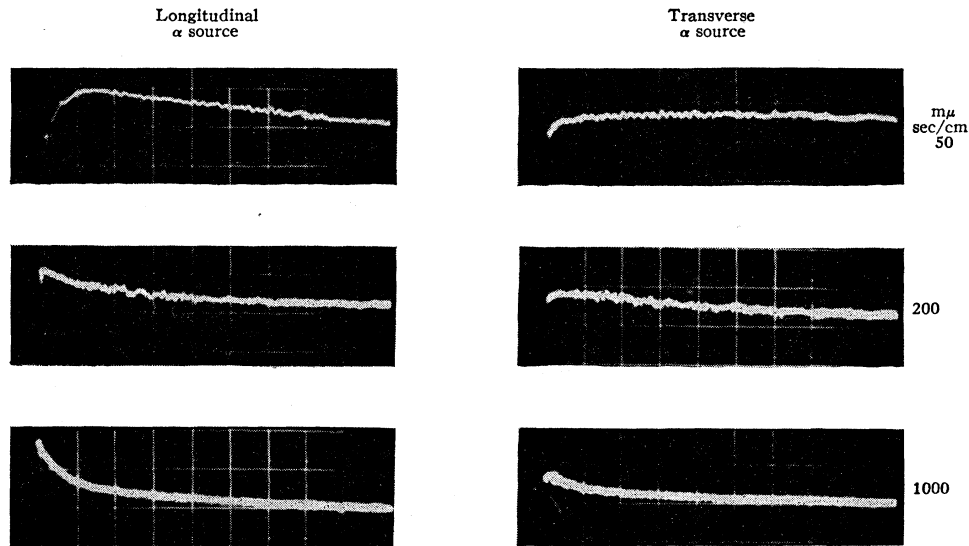


Fig. 6. Longitudinal and transverse α pulses in room air, 300 mm Hg, 2720 volts. Single sweeps at rates shown in margin

and to determine its velocity of propagation. Both the longitudinal α source (beam parallel to system axis) and the transverse source (beam perpendicular to system axis) were used for triggering purposes. In the case of the longitudinal source, the rise time of the pulse observed on the oscilloscope consists of the time for an α particle to travel the length of the cylinder, plus the time of formation of the electron avalanche created when the primary electrons ionize by collision in the high-field region near the central wire. With the transverse source, the pulse rise likewise contains the α -particle transit time, the time of formation of the initial avalanche, and in addition the time for the discharge to propagate down the length of the cylinder. The difference in rise time of the two types of pulses therefore yields the spreading time and, combined with the cylinder length, also the spreading velocity.

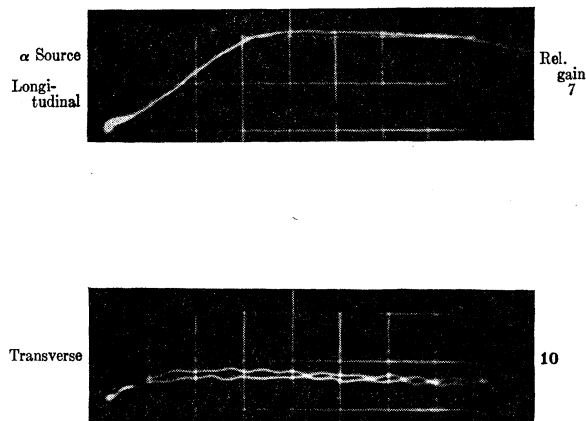


Fig. 7. Longitudinal and transverse α pulses in pure nitrogen, 300 mm Hg, 3000 volts, 20 m μ sec/cm sweep, single sweep.

Figure 6 shows some typical pulses observed in air at a pressure of 300 mm and applied potential of 2720 volts. It can be seen that the rise time for the transverse pulse is indeed noticeably greater than for the longitudinal pulse. Furthermore, there is approximately the same amount of total charge (proportional to the area under the pulse) in the two types of pulse, in spite of the fact that the initial ionization produced by a longitudinal α particle is approximately an order of magnitude greater than that from a transverse α particle. This lack of proportionality between initial ionization and total charge produced is to be expected, because additional multiplication occurs in the case of the transverse pulse when the discharge spreads along the wire.

As further confirmation that the effect was real, a similar set of measurements was made in pure nitrogen, for which it has been established that ionization in the gas is negligible and in which propagation along the wire is therefore not possible. One would thus expect the rise times for the transverse and longitudinal pulses to be about the same, and this was observed to be the case, as illustrated in Fig. 7. Rise time of the longitudinal pulse in the photograph was, in fact, slightly longer than that of the transverse, presumably because of imperfect collimation.¹⁹ Furthermore, without the additional ionization resulting from the spread of the discharge, the transverse pulse would be expected to contain a much smaller amount of total charge than the longitudinal. The total amount of charge contained in the two types of pulses was obtained by integrating the full pulses with slower sweep and was approximately proportional to the initial ionization in each case.

¹⁹ Lack of perfect collimation of the longitudinal beam caused some scatter in pulse rise times. These rarely exceeded a few times 10^{-8} sec, however, and for purposes of calculation the fastest rise was taken as representative of best collimation.

TABLE III. Velocity of spread in air.

p (mm Hg)	V (volts)	v (cm/sec)
100	1580	3×10^7
200	2190	3×10^7
300	2720	4×10^7
400	3240	6×10^7

Table III gives the values of the velocity of spread measured in air at four different pressures covering the observation range. The measured velocities of from 10^7 to 10^8 cm/sec agree in order of magnitude with values obtained by other investigators,²⁰⁻²² usually in typical Geiger counter fillings.

The pressure variation of the velocity is rather difficult to interpret, especially since at different pressures it was necessary to operate at different potentials. The velocity of spread depends on the time of formation of an electron avalanche and therefore on both the electron drift velocity and the distance from the wire at which electrons can first begin to ionize by collision; on the average lifetimes of the molecules in excited states; and on the average length, i.e., the absorbing free path for ionizing photons, and thus the total number of individual fictive²³ ionizing steps in the process.²⁰ These factors are no doubt all functions of pressure and/or voltage and are therefore hard to separate.

Since oxygen is responsible for the ionizing absorption of photons, the air was diluted with either nitrogen or oxygen to give different concentrations of oxygen. Then at a fixed total pressure it was also possible to work at the same voltage. The only factor one would expect to change radically in this case is the mean free path for photon absorption, which should decrease with increasing oxygen concentration. The difference between the fixed potential and the threshold for self-sustaining discharge, which changes slightly with O_2 concentration, is a minor factor.²³ The net result of increased O_2 concentration is shorter ionizing steps, a greater number of total steps, and hence a slower velocity of spread.²³ Table IV shows the variation of the spreading velocity with percentage of oxygen. In pure nitrogen there is no

TABLE IV. Variation of spreading velocity with percentage O_2 . $V = 2720$ volts, $p = 300$ mm Hg.

Percent O_2	v (cm/sec)
0	No spread
5	9×10^7
10	6×10^7
21	4×10^7
40	No α pulses

²⁰ Alder, Baldinger, Huber, and Metzger, *Helv. Phys. Acta* **19**, 207 (1946); **20**, 73 (1947).

²¹ H. Saltzmann and C. G. Montgomery, *Rev. Sci. Instr.* **21**, 548 (1950).

²² C. Balakrishnan and J. D. Craggs, *Proc. Phys. Soc. London* **A63**, 358 (1950).

²³ L. B. Loeb, following paper [*Phys. Rev.* **97**, 275 (1954)].



FIG. 8. Ion drift pulse in oxygen with amplification but with no secondary action, 300 mm Hg, 2775 volts, 1000 μ sec full scale, $RC = 3 \mu$ sec.

spread, as has been pointed out; the velocity decreases steadily as the percentage oxygen increases from 5 percent to 10 percent to 21 percent; finally at 40 percent oxygen it was no longer possible to observe the α pulses before the discharge became self-sustaining, and apparently in this region there is a transition to the streamer mechanism typical of pure oxygen as will be indicated.

Pure Oxygen

The nature of the various phenomena in pure O_2 seen on the oscilloscope as the voltage was raised is illustrated in Figs. 8-11 inclusive, for which the pressure was 300 mm.

Figure 8 shows the type of pulse observed when the applied voltage was relatively low—i.e., Townsend avalanches relatively small and little secondary mechanism. The duration of these pulses, as in N_2 , yields the mobility of the ions in O_2 , although the measurement is somewhat less precise than in nitrogen. The mobility extrapolated to 760 mm. and $20^\circ C$ was 2.2 ± 0.1 cm²/volt-sec. This is in satisfactory agreement with Varney's zero-field mobility of 2.25 ± 0.1 (at $0^\circ C$) as extrapolated from his data at higher E/p , for an ion he believes to be O_2^+ in accordance with Luhr's⁵ mass spectrographic studies.

A secondary mechanism became apparent, as in Fig. 9, at a somewhat higher voltage. These pulses again are of the *burst* pulse variety, and were also observed by Miller in pure oxygen at pressures of 200 mm and less. They differ from those of Fig. 8 in that their amplitude is higher, shape more irregular, and duration somewhat longer. The fluctuations are of much shorter duration and are orders of magnitude smaller than the burst pulses of Fig. 5. Electron attachment to oxygen molecules near the cathode and subsequent detachment in the high-field region might account for the extension in duration and for some irregularity in pulse shape. The observed irregularities, however, are in principle localized discharges of the burst pulse type, triggered by negative ions but unable to propagate down any length of wire because of high absorption of photons. The large numbers of negative ions could not by



FIG. 9. Burst pulses in oxygen, 300 mm Hg, 2900 volts, 1000 μ sec full scale, $RC = 3 \mu$ sec. Single sweep.

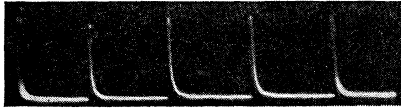


FIG. 10 Streamers in oxygen, 300 mm Hg, 3050 volts, 1000 μ sec full scale, $RC=3 \mu$ sec. Single sweep—gain 1/200 that on Fig. 9.

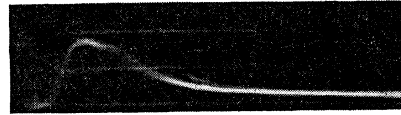


FIG. 11. Streamers in oxygen, 300 mm Hg, 3050 volts, 1 μ sec full scale, $RC=0.003 \mu$ sec. Many sweeps superposed.

statistical effect account for the fluctuations. Because of their limited spread, the fluctuations are smaller in amplitude than they were in air. These pulses were observed, at the appropriate V , at all pressures in pure oxygen, with smaller ones present even without the α -particle triggering. They represent an important phenomenon setting a lower limit to velocity of pulse propagation, as shown by Loeb.²³

Figure 10 illustrates another type of pulse observed at still higher applied voltages. These were present at pressures of 200 mm and above, and required no α triggering for their initiation. They differed markedly from the burst pulses in several respects: Their amplitude was much higher (gain in Fig. 10 is less by a factor of 200 than in Fig. 9). They were spaced at uniform intervals of time and were approximately constant in amplitude at a given V and p . Their duration, as can be seen in Fig. 11 with a faster sweep speed, was a great deal shorter (10^{-7} sec as opposed to 10^{-4}). Instantaneous currents in these pulses were as high as 10^{-4} amp, and it is estimated (from the pulse area of Fig. 11) that they contain approximately 10^8 electrons.

These properties are characteristic of streamers, which like the burst pulses were originally observed in point-to-plane geometry^{17,18} and were suspected to have been observed by Miller and Loeb.³ These oscillograms and data for the first time consequently indicate the existence of streamers in Geiger counter geometry. The basic processes in streamer formation have been described by Loeb.²⁴ The discharge spreads in a series of steps very similar to those involved in the spread along

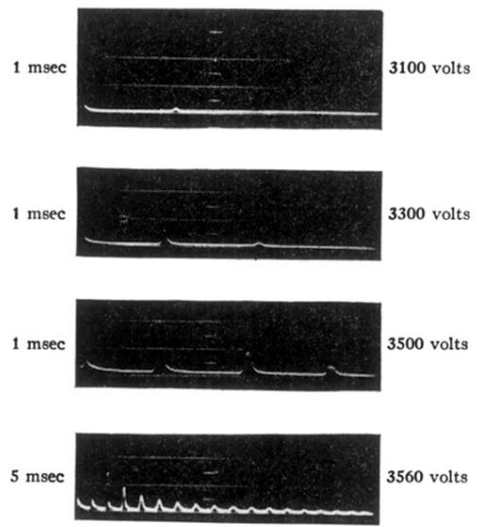
the wire in air, except that for streamers the propagation is radially outward toward the cathode instead of along the axis. The outward direction for the propagation is favored by extremely localized photoionization, i.e., when the steps become very short.

It is interesting to note on comparison of Figs. 8 and 10 that streamer spacing is closely related to ion transit time. At all pressures where they were observed, streamers were separated by intervals equal to roughly $\frac{2}{3}$ of the duration of the single ion pulse appearing at lower voltages. Ion transit times are shorter in the streamer region than for ion drift pulses, both because the applied voltage is higher and because of much denser space charge increasing cathode fields. It appears, therefore, that the ions in one streamer which are created closest to the wire must travel essentially all the way to the cathode before the field recovers sufficiently for a second streamer to begin. It is in fact possible that the arrival at the cathode of positive ions created in one streamer actually results in the liberation of secondary electrons which serve to trigger the next streamer as observed by A. F. Kip in point-to-plane corona with a screening gauze over the cathode.

ACKNOWLEDGMENTS

The writer wishes to thank Professor L. B. Loeb, who proposed this investigation, including the use of the transverse pulse, and under whose guidance this work was carried out, for his encouragement and suggestions. Special thanks are also due to Professor J. H. Reynolds and Mr. S. Balestrini for the mass spectrographic analyses, and to Mr. M. Corbett for his expert assistance in glassblowing.

²⁴ L. B. Loeb, *Fundamental Processes of Electrical Discharge in Gases* (John Wiley and Sons, Inc., New York, 1939).



Nitrogen—400m

FIG. 1. Secondary ion pulses in pure nitrogen, 400 mm Hg,
 $RC=3 \mu\text{sec}$; single sweep.



FIG. 10 Streamers in oxygen, 300 mm Hg, 3050 volts, 1000 μ sec full scale, $RC=3 \mu$ sec. Single sweep—gain 1/200 that on Fig. 9.

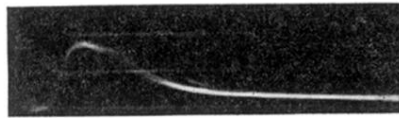


FIG. 11. Streamers in oxygen, 300 mm Hg, 3050 volts, 1 μ sec full scale, $RC=0.003 \mu$ sec. Many sweeps superposed.

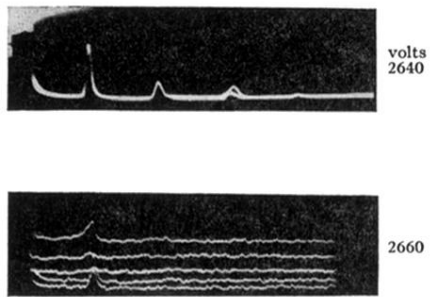


FIG. 2. Secondary ion pulses, top trace, and self-sustaining discharge in pure nitrogen, 200 mm Hg, 1000 μ sec full scale, $RC = 3 \mu$ sec. Upper trace—a few superposed sweeps. Lower trace—several single sweeps separated by vertical displacement showing initial and secondary with self-sustaining fluctuation.

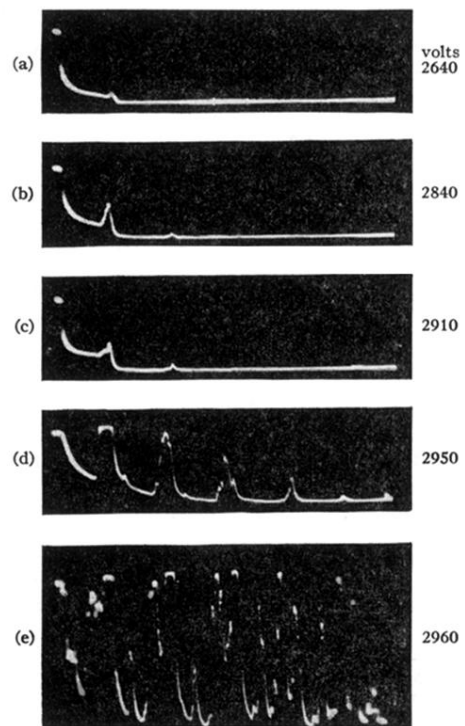


FIG. 3. Secondary ion pulses and self-sustaining discharge in nitrogen plus 5 percent oxygen, 200 mm Hg, 1000 μ sec full scale, $RC=3 \mu$ sec. Traces such as *d* and *e* are single sweeps.

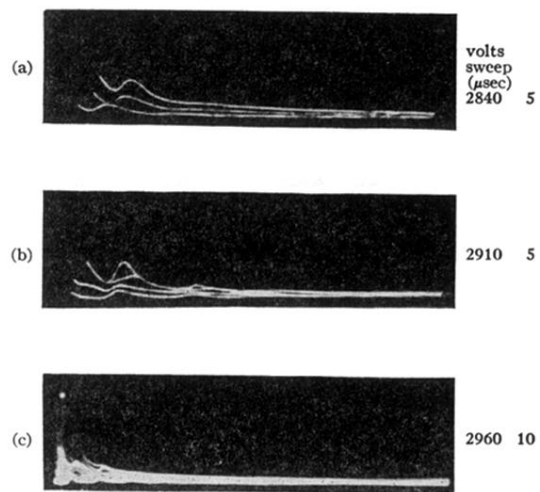


FIG. 4. Secondary photoelectric pulses in nitrogen plus 5 percent oxygen, 200 mm Hg, $RC=0.03 \mu\text{sec}$. Several sweeps indicate lack of accurate reproducibility and that at self-sustaining corona in trace (c) the photon γ_p does not sustain itself as a discharge.

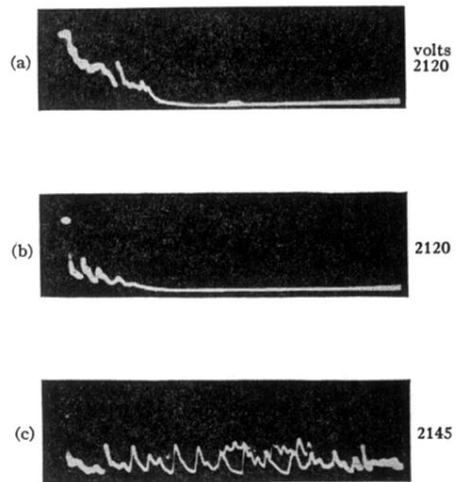


FIG. 5. Burst pulses and self-sustaining discharge in nitrogen—20 percent oxygen mixture, 200 mm Hg, 1000 μ sec full scale, $RC=3 \mu$ sec. Gain is down by a factor of 10 in (c). Single sweeps, except part of a second sweep in (c).

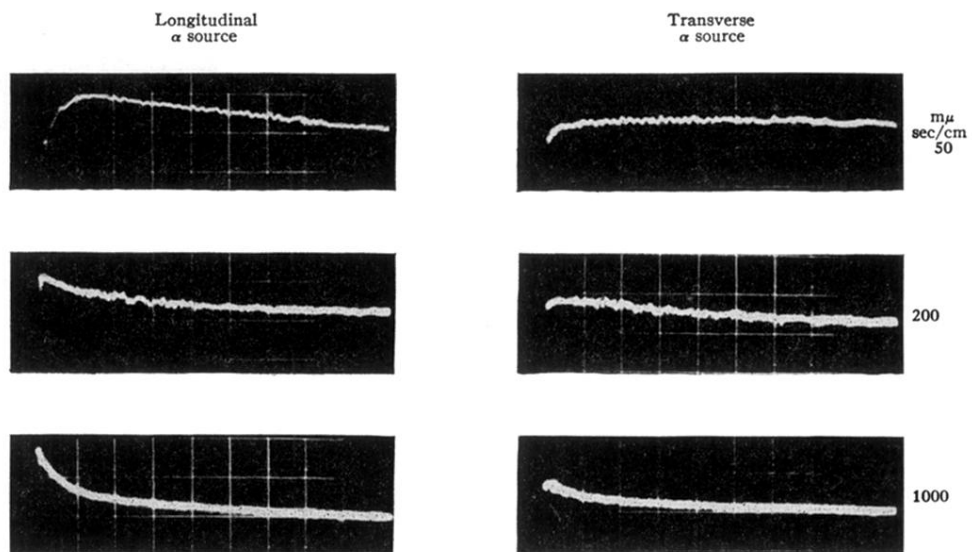


FIG. 6. Longitudinal and transverse α pulses in room air, 300 mm Hg, 2720 volts.
Single sweeps at rates shown in margin

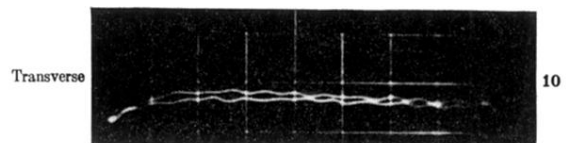
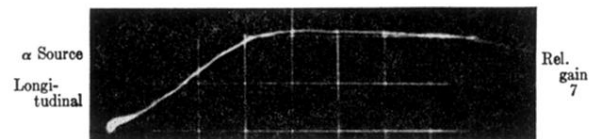


FIG. 7. Longitudinal and transverse α pulses in pure nitrogen, 300 mm Hg, 3000 volts, 20 m μ sec/cm sweep, single sweep.



FIG. 8. Ion drift pulse in oxygen with amplification but with no secondary action, 300 mm Hg, 2775 volts, 1000 μ sec full scale, $RC=3 \mu$ sec.

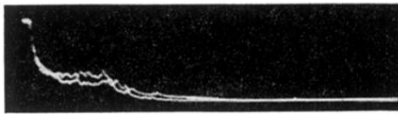


FIG. 9. Burst pulses in oxygen, 300 mm Hg, 2900 volts, 1000 μ sec full scale, $RC=3 \mu$ sec. Single sweep.